



# Online electrochemistry coupling liquid chromatography-mass spectrometry for rapid investigation on the phase I and phase II simulated metabolic reactions of flavonoids

Yanyan Niu<sup>1</sup> · Yuxue Chen<sup>1</sup> · Juan Zhou<sup>1</sup> · Wei Sun<sup>1</sup>

Received: 4 January 2024 / Revised: 20 February 2024 / Accepted: 26 February 2024 / Published online: 7 March 2024  
© The Author(s), under exclusive licence to Springer-Verlag GmbH, DE part of Springer Nature 2024

## Abstract

In this study, an online electrochemistry coupling high-performance liquid chromatography-mass spectrometry (EC-HPLC-MS) technology has been developed for simulating metabolic reactions and rapid analysis of metabolites of flavone, quercetin, and rutin, which are not only widely present compounds with pharmacological activity in nature, but also have structural similarity and variability. The simulated metabolic processes of the substrates (phase I and phase II metabolism) were implemented on the surface of glassy carbon electrode (GCE) by using different electrochemical methods. After online chromatographic separation, the products were transmitted to a mass spectrometer for detection, in order to speculate relevant reaction pathways and structural information of the reaction product. The main metabolites, including methylation, hydroxylation, hydrolysis, and conjugation reaction products, had been successfully identified through the designed in situ hyphenated technique. Furthermore, compared with metabolites produced by in vitro incubation of rat liver microsomes, it was found that the products of electrochemical simulated metabolism were more abundant with diverse metabolic pathways. The results indicated that the proposed method exhibited advantages in the sample pretreatment process and detection cycle without compromising the reliability and accuracy of the results.

**Keywords** Oxidative metabolism · Electrochemical simulation · Flavonoids · Glutathione · Conjugation reaction · In vitro incubation

## Introduction

Electrochemical technology is a flexible and controllable classical chemical reaction measure, which is therefore considered as an effective screening tool for exploring the potential oxidative or reductive metabolism of drugs [1–3]. Undoubtedly, monitoring the metabolic process of drugs is beneficial for guidance of clinical medication effectively and safely [4]. At present, traditional drug metabolism research employs in vivo experiments using animal models or in vitro

experiments using liver microsomes incubation [5, 6]. The main drawbacks are complex sample processing, long experimental cycles, and high costs. Therefore, a convenient and agile technology for electrochemical simulation of enzyme catalyzed drug metabolism has gradually developed and improved. It combines efficient and flexible electrochemical technique with chromatography owing excellent sample separation capability, and mass spectrometry possessing powerful compound structure analysis function, achieving targeted synthesis of drug metabolites, prediction of metabolic processes, and monitoring of potential metabolites and active intermediates in real-time with advantages of simple methods, high analysis efficiency, and high sensitivity [7–9]. Yang et al. [10] developed an electrochemical microreactor technique for rapid analysis and identification of flavonoid and organic acid metabolites in Hawthorn by using an online electrochemical microreactor combined quadrupole time-of-flight (Q-TOF) tandem mass spectrometry, which can be applied to simulate the oxidative metabolism of active ingredients and product analysis in food. Szultak-Mlynska et al.

✉ Yanyan Niu  
070080@hainnu.edu.cn

<sup>1</sup> Hainan Engineering Research Center of Tropical Ocean Advanced Optoelectronic Functional Materials, Key Laboratory of Laser Technology and Optoelectronic Functional Materials of Hainan Province, Key Laboratory of Functional Materials and Photoelectrochemistry of Haikou, College of Chemistry and Chemical Engineering, Hainan Normal University, Haikou 571158, China

[11] established an electrochemical analysis method coupled with liquid chromatography and tandem mass spectrometry (LC-MS) to study the oxidation products of immunosuppressants. Due to its potential to simulate numerous oxidation reactions, electrochemical technology had become an alternative method for generating and detecting metabolites in drug development, providing a good approximation of metabolic processes that occur in vivo. Yue et al. [12] investigated the oxidation products and metabolic pathways of five Citrus flavonoids by online electrochemical/quadrupole time-of-flight mass spectrometry (EC/Q-TOF/MS), and the structures of metabolites were determined by precise mass as well as reported literature. It may be expected to become an effective approach to study the metabolic transformation of complex food components.

Flavonoids are a kind of secondary metabolites widely existing in plants with antioxidant biological activity [13]. They can prevent damage caused by free radicals through clearing reactive oxygen species, activating antioxidant enzymes and so on, and have good pharmacological activity for cardiovascular disease or atherosclerosis disease [14, 15]. Figure 2A shows the basic skeleton nucleus of flavonoids, consisting of two benzene rings that connected by a pyrane ring, with a characteristic double bond of C<sub>2</sub>-C<sub>3</sub>. The bioactivity of flavonoids mainly depends on the structure of substituent groups in the C6-C3-C6 rings [13, 16, 17]. The biological metabolic process generally includes two stages: Phase I metabolism is mainly a redox reaction catalyzed by cytochrome P450 in the liver, including oxidation, demethylation, hydrolysis, and other reactions. Phase II metabolism refers to the conjugation reaction between drugs or phase I metabolites and endogenous substances such as glutathione (GSH), glucuronic acid, or sulfate [18, 19]. With the metabolism and structural changes of drugs in organisms, the pharmacological activities gradually decrease or even disappear. As a result, it is of great significance for research on drug metabolism in many fields such as new drug development, drug design, drug safety, and drug toxicity [20–23].

In this research, flavonoid compounds with the same skeleton structure (flavone, quercetin, and rutin) are selected as the research subjects. Flavone represents the basic backbone structure of the selected substances and serves as a control. Quercetin is the glycoside of rutin, of which have partial similarities in structure, but also respective characteristics. They are not only widely present compounds with pharmacological activity in nature, but their characteristic structures may also represent a certain type of metabolic transformation process. The phase I oxidative metabolism and phase II conjugation reaction that introduce GSH as an endogenous compound or capture agent were simulated by online hyphenation of electrochemistry with high-performance liquid chromatography-mass spectrometry (EC-HPLC-MS) method, and the corresponding metabolites of

possible metabolic pathways had also been explored and elaborated in detail. Furthermore, rat liver microsomes were used to conduct in vitro incubation experiment on the target analytes. The incubated products were detected by offline HPLC-MS to verify the feasibility and reliability of this online electrochemical simulation of biological metabolism technology.

## Experimental

### Reagents and materials

Ammonium acetate (CH<sub>3</sub>COONH<sub>4</sub>, ≥99.0%), formic acid (99%), acetic acid (99.5%), ammonia solution (30.0%), flavone, quercetin, rutin, magnesium chloride (MgCl<sub>2</sub>, 99.0%), β-nicotinamide adenine dinucleotide phosphate (β-NADPH, 95%), glutathione (GSH, 98%), and phosphate buffer solution (PBS, 1×, pH 7.2–7.4) were purchased from Shanghai Aladdin Bio-Chem Technology Ltd. Co. (Shanghai, China). Acetonitrile (CH<sub>3</sub>CN, for LC-MS) and methanol (CH<sub>3</sub>OH, for LC-MS) were offered by Merck Chemicals (Shanghai, China). Rat liver microsomes (RLM, male Sprague Dawley rats) were obtained from Thermo Fisher Scientific Inc. (USA). Ultrapure water was supplied by Milli-Q IQ 7000 (Merck Millipore, Germany) with resistivity as 18.5 MΩ·cm and used during the whole experiments. The microsomes were stored at –70 °C before use.

### Electrochemical conditions

The electrochemical simulation experiments were carried out on the assembled thin-layer electrochemical flow cell (Bioelectro Analytical Science Inc., Japan) online hyphenated to a Q Exactive Focus high-resolution mass spectrometer (HRMS, Thermo Fisher Scientific Inc., USA) or a HPLC-HRMS system equipped with UltiMate 3000 (Thermo Fisher Scientific Inc., USA). The electrochemical workstation (IGS 1130, Guangzhou Ingsens Sensor Technology Ltd. Co., China) was connected to the electrochemical flow cell, which consisted of a three-electrode system including a glassy carbon working electrode (GCE, Φ=3 mm), an Ag/AgCl reference electrode, and a hollow stainless steel pipe (1 mm i.d.) as the auxiliary electrode. Before the experiment, the GCE surface was polished carefully and washed by ultrapure water. The target solution was slowly injected into the electrochemical flow cell at room temperature through a peristaltic pump equipped with a 500 μL syringe at a flow rate of 10 μL/min. A series of variable or constant potential controls were implemented on the electrochemical flow cell to simulate biological metabolism.

## Liquid chromatography conditions

The complex reaction products were separated and purified through an online UltiMate 3000 HPLC system equipped with a quaternary pump, a column temperature chamber, and an autosampler. The analysis was carried out on a HyperSil GOLD C18 reversed phase column (3  $\mu\text{m}$ , 100 mm $\times$ 2.1 mm) with 0.1% formic acid solution (A) and methanol (B) as mobile phase. The column temperature was 25  $^{\circ}\text{C}$  and the flow rate was 0.2 mL/min. The gradient elution approach was applied with the mobile phase gradient as follows: 0–5 min, 10% B; 5–17 min, 10–50% B; 17–30 min, 50–100% B.

## Mass spectrometry conditions

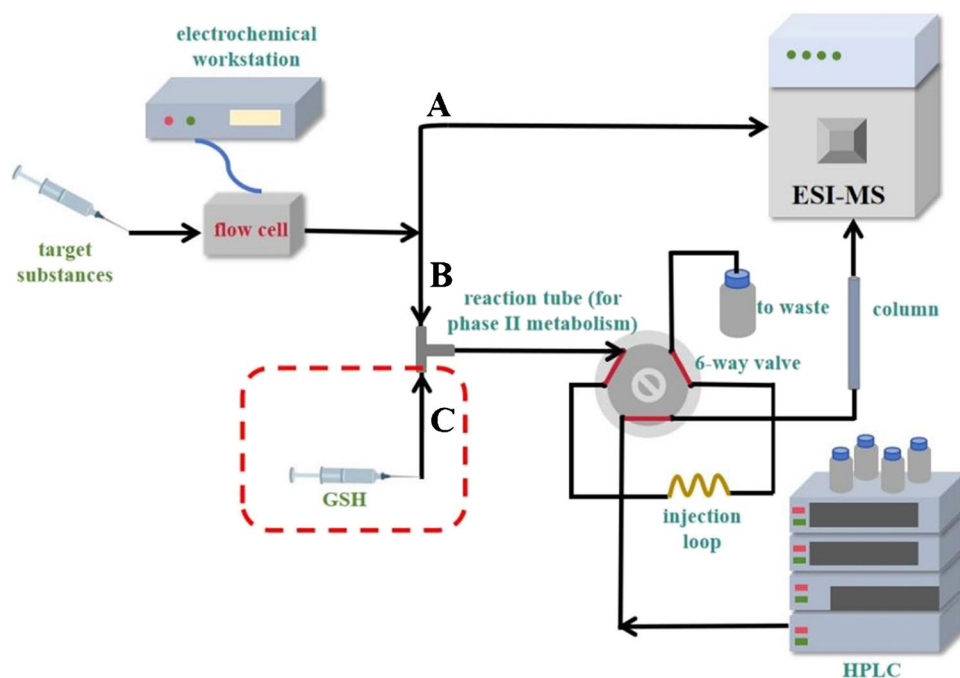
The biological metabolism simulated by electrochemistry was analyzed by EC-MS (Fig. 1, path A) or EC-HPLC-MS (Fig. 1, paths B and C) through different potential controls, while the metabolites incubated through rat liver microsomes *in vitro* were determined using offline HPLC-MS. The above experiments were performed on a high-resolution mass spectrometer (HRMS, Q Exactive Focus, Thermo Fisher Scientific Inc., USA) equipped with an ESI ion source and the electrospray parameters were as follows: spray voltage 4.1 kV in positive ion mode and 3.8 kV in negative ion mode, capillary temperature 330  $^{\circ}\text{C}$ , sheath gas 25 arb, aux gas 10 arb, and probe heater temperature 300  $^{\circ}\text{C}$ , respectively. The ion mode was determined based on the properties of the samples with the mass range recording as  $m/z$  100–800.

## Preparation of substrates and electrochemistry simulation

A 4.0 mmol/L ammonium acetate solution prepared by methanol/water (80/20, v/v) was used as the basic electrolyte and pH was adjusted to 7.4. Then a 0.1 mmol/L target standard solution was made up by using the basic electrolyte. All the above solutions were filtered with a 0.22  $\mu\text{m}$  membrane before injection into the mass spectrometer.

In electrochemical simulation of phase I oxidative metabolism, one method was introducing the electrolytic products of the substrates into the mass spectrometer after linear sweep voltammetry (LSV) for real-time monitoring, and constructing an EC-MS analysis system with electrolyte flow rate as 10  $\mu\text{L}/\text{min}$  and scanning speed as 10 mV/s, which ensured complete oxidation of the targets (Fig. 1, path A). Alternatively, a constant potential scanning method was used to introduce quantitative electrolytic products (10  $\mu\text{L}$ ) into online HPLC-MS for determination, and the applied potential varied depending on the electrochemical properties of the target substances, which was known as the EC-HPLC-MS analysis method (Fig. 1, path B). In electrochemical simulation of phase II metabolism, GSH was dissolved in ammonium acetate solution (4.0 mmol/L) at a concentration of 0.1 mmol/L and was considered as an endogenous compound, which was further introduced into a 1.5 m long reaction tube with the phase I metabolites simultaneously at the same flow rate through a T-shaped tee (Fig. 1, paths B and C). It may trigger a conjugation reaction between GSH and the targets or phase I metabolites, and the products were determined by the online HPLC-MS. The schematic diagram

**Fig. 1** Schematic diagram of online coupling devices: EC-MS for phase I metabolism (path A), EC-HPLC-MS for phase I (path B), and phase II metabolism (merging path of B and C)



of the construction process of simulated phase I and phase II metabolism is depicted in Fig. 1.

### Preparation of metabolites by using liver microsomes incubation

The target substances were also incubated with rat liver microsomes *in vitro* by using 50 mmol/L phosphate buffer solution (pH 7.4) as the culture medium. In the phase I metabolism experiment, the target substance (0.1 mmol/L) and liver microsomes (1.5 mg/mL) were added to phosphate buffer solution for preincubation at 37 °C for 5 min. Then MgCl<sub>2</sub> and β-NADPH were added with final concentrations as 0.5 mmol/L and 1.2 mmol/L, resulting in a mixture with a total volume of 0.5 mL. Afterwards, the mixed solution was incubated in water bath at 37 °C for 90 min, and then an equal volume of acetonitrile was added to terminate the reaction. The final solution was fully shaken and centrifuged at 13,000 rpm for 5 min, followed by filtration using a 0.22 μm

microporous membrane. In the phase II metabolism experiment, GSH was added to the phosphate buffer solution along with the target substance and liver microsomes in the first step. The subsequent incubation process and sample preparation repeated the steps of the phase I metabolism experiment. All treated samples were analyzed by using offline LC-MS.

## Results and discussion

### Electrochemical characteristics of the target substances

The electrochemical oxidation characteristics of flavone, quercetin, and rutin were investigated in both static and dynamic electrolytic cell with the results shown in Fig. 2. These compounds have a typical C6-C3-C6 skeleton structure that connects two benzene rings through three carbons chain, where

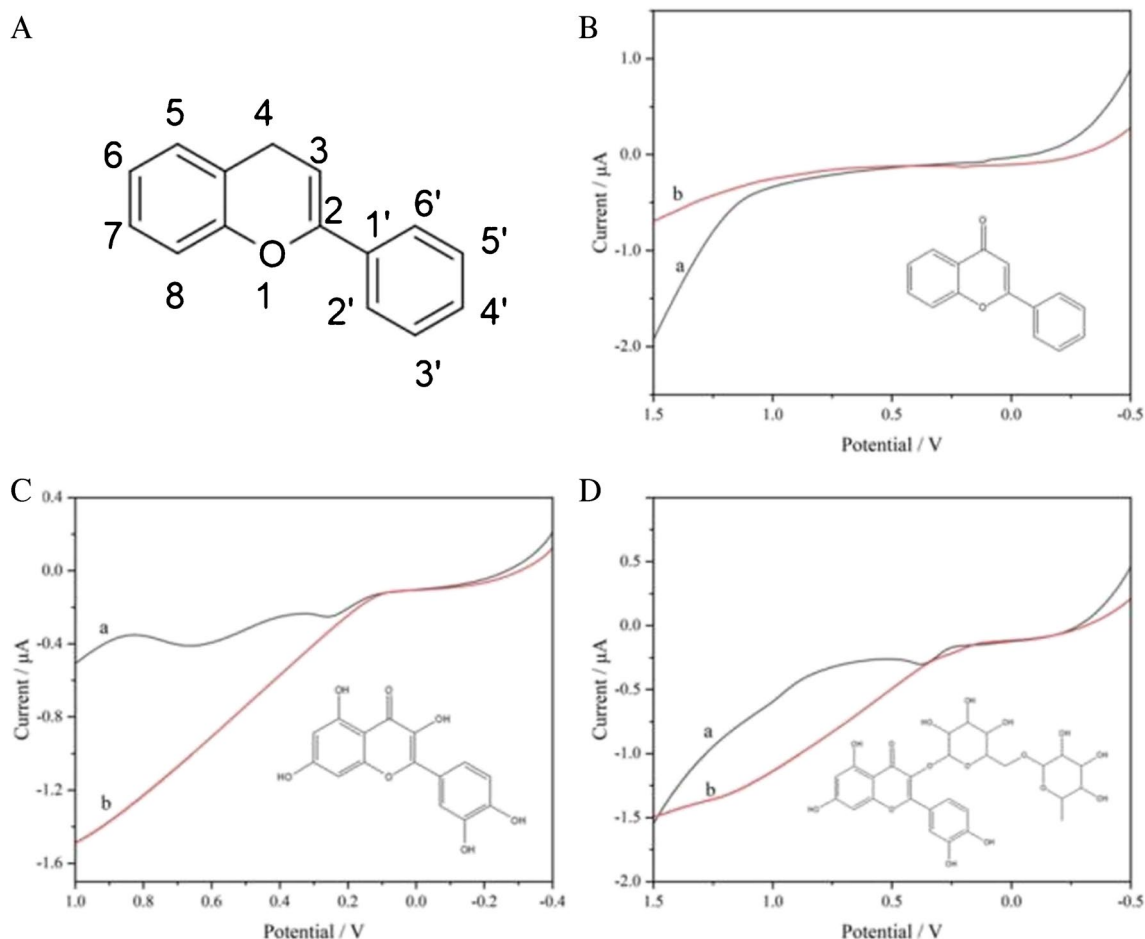


**Fig. 2** A Skeleton nucleus of flavonoids. LSV curves of **B** flavone, **C** quercetin, and **D** rutin in static (curve a in each figure with a flow rate of 0 μL/min) and dynamic (curve b in each figure with a flow rate of 10 μL/min) electrolytic cells, respectively

quercetin and rutin have abundant hydroxyl groups. Obviously, the LSV curve of flavone in a static electrolytic cell with the electrolyte being stationary (flow rate of 0  $\mu\text{L}/\text{min}$ ) was smooth and peak free (Fig. 2B, curve a), while quercetin and rutin exhibited significant oxidation peaks (curve a in Fig. 2C and D, respectively), indicating that the presence of active hydroxyl groups provided multiple possibilities for substrate oxidation. It is worth noting that the oxidation peaks of quercetin and rutin disappeared in the dynamic electrolytic cell with electrolyte flow rate of 10  $\mu\text{L}/\text{min}$  to be replaced by a continuous increase in current at the potential where the oxidation peaks vanished (curve b in Fig. 2C and D). It indicated continuously updated substrate on the electrode surface in the flowing electrolyte, resulting in a continuous increase in current.

### Online monitoring of the electrochemical oxidation process of quercetin by EC-MS

Initially, three electrochemical methods including LSV, differential pulse voltammetry (DPV), and square wave voltammetry (SWV) were used to investigate the changes in the electrochemical oxidation products of quercetin by online EC-MS without HPLC separation and the results are shown in Fig. 3A. It was found that the extracted ion chromatogram (EIC) peak intensity of  $m/z$  331.0450 (considered as methoxylation product of quercetin) from LSV electrochemical oxidation products was stronger than that of DPV and SWV at the same substrate concentration and electrolyte flow rate, indicating a higher reaction efficiency of LSV. Therefore, LSV was selected as a potential scanning method to simulate oxidation metabolism.

Furthermore, the phase I oxidative metabolites of quercetin simulated by LSV mode were determined by using online EC-MS. The potential increased from  $-0.1$  to  $1.3$  V with a scanning rate of  $10$  mV/s and the MS recorded from  $100$  to  $450$  Da in the negative ion mode. The 3D mass voltammogram in Fig. 3B showed the variation of quercetin ion peak ( $[\text{M}-\text{H}]^-$  at

$m/z$  301.0345) and product ion peaks with oxidation potential. The curves of ion intensity ratio of products to quercetin ( $I_p/I_0$ ) versus applied voltage in Fig. 3C also indicated the occurrence of quercetin oxidation behavior at around  $0.6$  V, and the relative variation ratio of product 363.0713 was the most significant. With the continued increasing of potential, the  $I_p/I_0$  of products 363.0713, 331.0450, and 349.0556 reached maximum at  $1.2$  V. However, considering the possibility of water electrolysis at a high potential, the voltage applied in subsequent experiments was determined to be  $1.0$  V. The ion peaks observed at  $m/z$  331.0450 and 349.0556 were implied methoxylation and further hydrolysis of quercetin. Although the variation of electrochemical reaction products with potential can be monitored by LSV mode, the continuously changing potentials and constantly updating electrolytes may cause incomplete electrolysis and ignore some trace products information. In addition, it was found that the continuous injection of electrochemical reaction products generated by linear potential scanning would easily cause blockage of the ion source injection needle, which not only caused irregular changes in ion detection, but also increased the risk of equipment damage. Considering the complexity of the unseparated electrochemical products, the experimental process was redesigned by using quantitative injection of electrolytic products, followed by chromatographic column separation and purification, and then introducing to mass spectrometer for detection. It not only effectively avoids the above issues, but also improves the efficiency and accuracy of sample analysis. Therefore, the subsequent discussion will revolve around this design approach.

### Online monitoring of simulated oxidative metabolites by EC-HPLC-MS

Due to the low concentration of electrolytic products in continuous linear potential scanning, some oxidation products information may be ignored. Therefore, constant potential

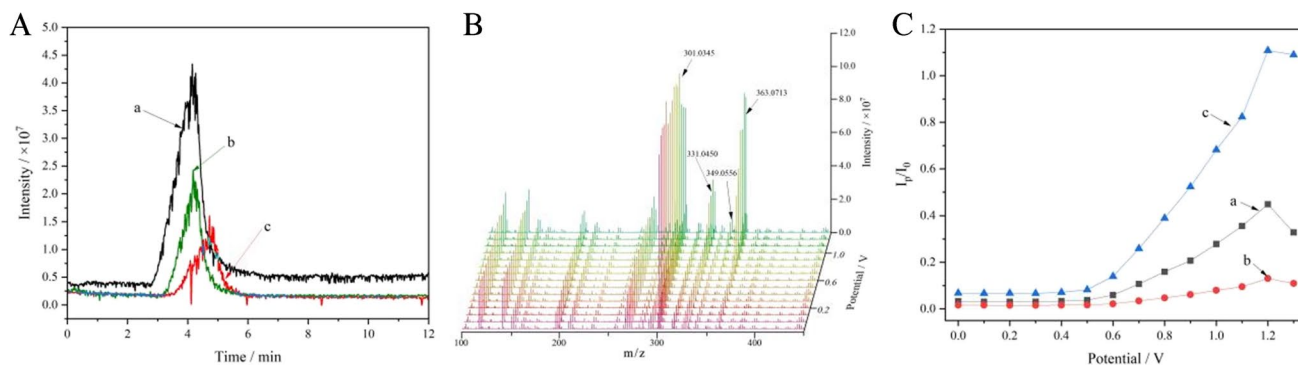


**Fig. 3** **A** Extracted ion chromatograms of quercetin oxidation product ( $m/z$  331.0450) by (a) LSV, (b) SWV, and (c) DPV with a potential range of  $-0.1$  to  $1.3$  V. **B** 3D mass voltammograms of the electro-

chemical oxidation of quercetin. **C** The curves of ion intensity ratio of products (a to c:  $m/z$  331.0450, 349.0556, and 363.0713) to quercetin ( $m/z$  301.0345) versus applied voltage

scanning combined with online HPLC-MS analysis was implemented in this paper, which was beneficial for improving the sensitivity of detection [24, 25]. Phase I oxidation metabolites simulated through potentiostatic scanning were trapped in a sample loop (10  $\mu$ L) by switching a six-way valve, and shifted to the HPLC system after complete and sufficient reaction, achieving a continuous process of online reaction, separation, detection, and characterization. Similarly, the simulation of phase II metabolism involved introducing GSH into the phase I metabolites and further isolating of products for MS analysis.

## Flavone

Firstly, phase I oxidative metabolism of flavone was simulated at a constant potential of 1.0 V, and the products were determined by online HPLC-MS. As it turned out, no obvious oxidation product peak was observed except for the significant ion peak of flavone. Due to the lack of active hydrogen, electrochemical property of flavone is relatively stable, which is consistent with the characterization result

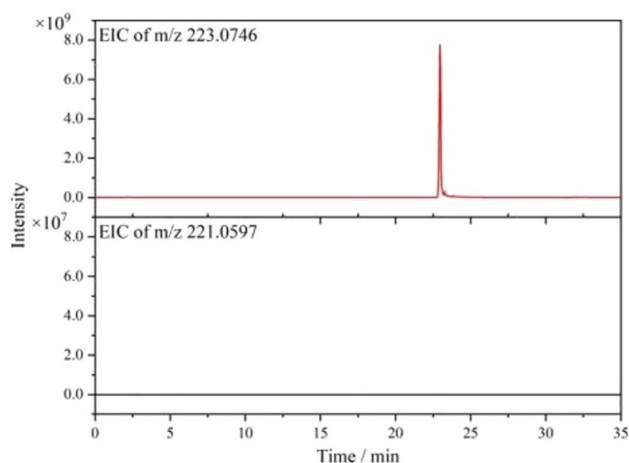


**Fig. 4** Extracted ion chromatogram (EIC) of flavone after electrochemical oxidation at 1.0 V by EC-HPLC-MS

in Fig. 2B. In addition, due to the nucleophilicity of flavone carbonyl oxygen, there was a significant extracted ion peak in positive ion mode (see Electronic Supplementary Material Fig. S1A), while no corresponding extracted ion peak for negative ion mode was observed (Fig. 4).

Glutathione (GSH) conjugation reaction is a common type of phase II metabolic reaction. GSH is a tripeptide of glutamate, cysteine, and glycine, containing an active thiol group (-SH) which is easily oxidized and dehydrogenated, making it nucleophilic [26, 27]. Due to its specific structure, it proved to be the free radical scavenger in the body, and can also chelate with heavy metals or bind with electrophilic toxins, reducing the toxicity of drugs or metabolites [28, 29]. In order to further simulate and elucidate the phase II metabolism and metabolic pathways of the substrates, the conjugation reaction of phase I metabolites and GSH was implemented through online EC-HPLC-MS, which can be considered as a simulation approach of phase II metabolic reactions. Similarly, as a result of the lack of active groups in flavone and absence of significant oxidation products during the electrochemical simulation of phase I metabolism reaction (such as hydroxylated, methylated products), no obvious oxidation product was detected during the simulation of phase II metabolism reaction.

## Quercetin

Unlike flavone, quercetin contains multiple hydroxyl groups, resulting in abundant oxidation products. Figure 5A shows the online HPLC-MS detection results of quercetin with and without potential application. Due to the presence of active hydrogen atoms in quercetin, the response in negative ion mode was stronger than that of positive ion mode (with MS spectra in negative ion mode shown in Electronic Supplementary Material Fig. S1B). Furthermore, the response of quercetin ( $m/z$  301.0345) oxidized at 1.0 V is significantly decreased, indicating the occurrence of an oxidation reaction. The EICs of quercetin simulated phase I oxidative metabolites are shown in Fig. 5B. Three extracted ion peaks

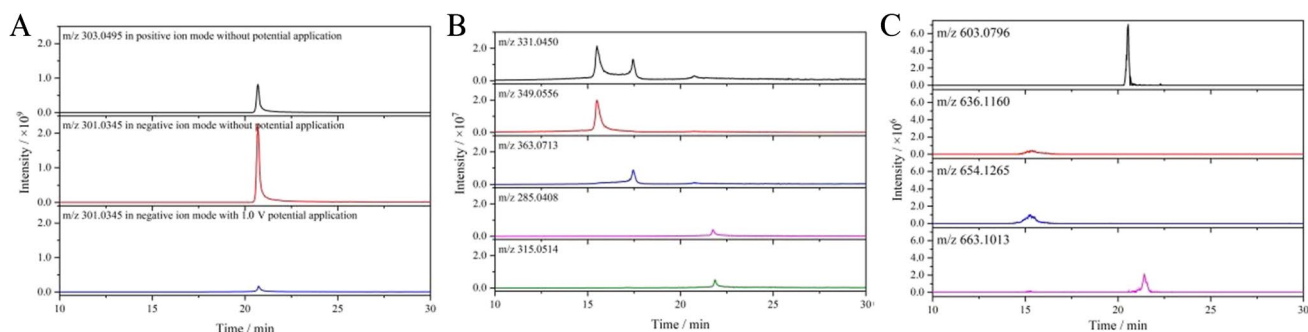


**Fig. 5** EICs of **A** quercetin, **B** simulated phase I metabolites, and **C** simulated phase II metabolites conjugated with GSH by electrochemical oxidation at 1.0 V through EC-HPLC-MS

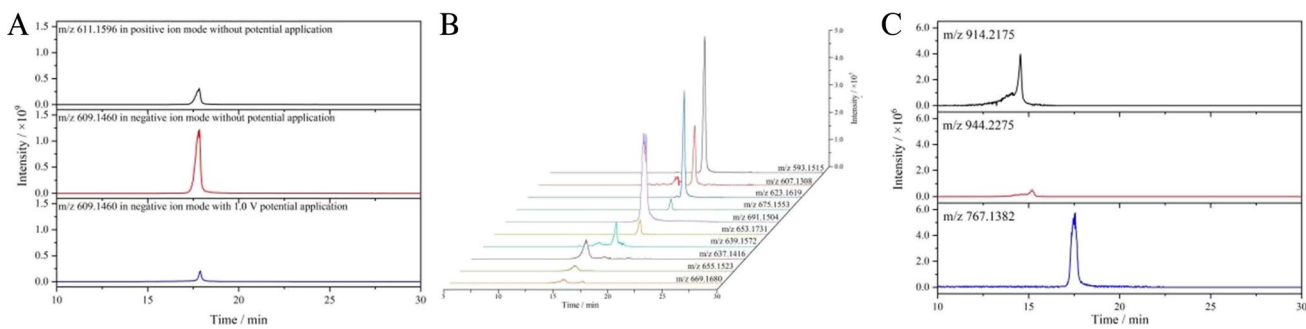


**Fig. 6** EICs of **A** rutin, **B** simulated phase I metabolites, and **C** simulated phase II metabolites conjugated with GSH by electrochemical oxidation at 1.0 V through EC-HPLC-MS

at  $m/z$  331.0450, 349.0556, and 363.0713 can be significantly observed. The ion peak of  $m/z$  331.0450 was quercetin methoxylated products, which contained two peaks that may originate from different reaction sites in the quercetin structure with different polarities, while the ion peak of  $m/z$  363.0713 represented methanol adduct of the product of

$m/z$  331.0450. The product ion of  $m/z$  349.0556 was 18 Da greater than  $m/z$  331.0450, indicating further hydrolysis of methoxylated quercetin. In addition, two weaker ion peaks of  $m/z$  315.0514 and 285.0408 were also shown, implying the typical methylation and dehydroxylation products of quercetin respectively. Furthermore, the spectra in  $MS^2$  by

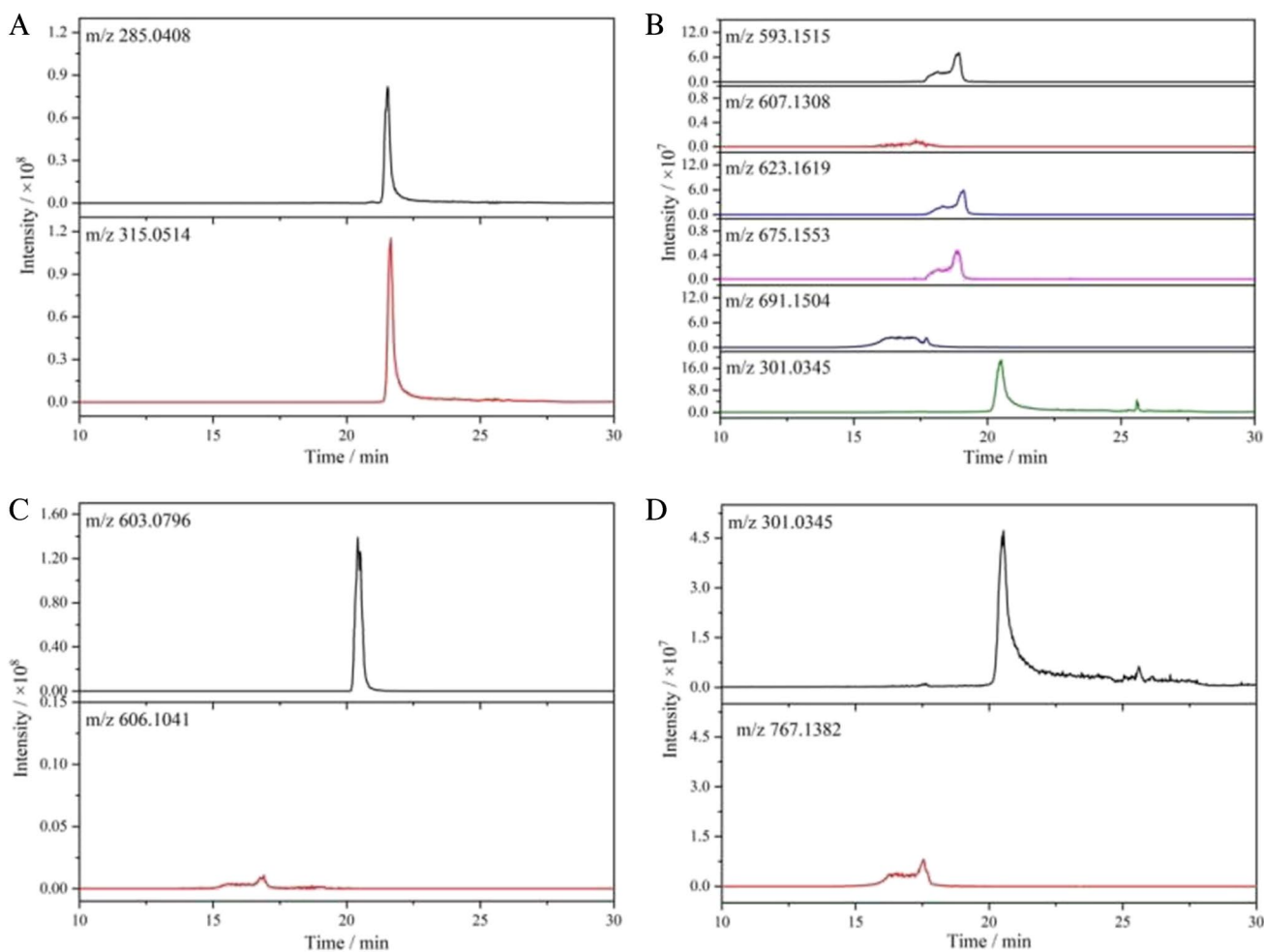


**Fig. 7** EICs of quercetin and rutin metabolites incubated in vitro liver microsomes. Phase I metabolites of **A** quercetin and **B** rutin; phase II metabolites of **C** quercetin and **D** rutin

collision induced dissociation of the main oxidation products at  $m/z$  331.0450, 349.0556, and 363.0713 were achieved with their structures inferred in Electronic Supplementary Material Fig. S5 and S6.

In the electrochemical simulation of phase II metabolism, the oxidized target substance is mixed with GSH solution to obtain the conjugated product. There were mainly four adducts formation between quercetin oxidation products and GSH with the result shown in Fig. 5C. The ion peak of  $m/z$  603.0796 might be attributed to the addition of dehydrogenated quercetin to GSH. Meanwhile, two weak extracted ion peaks were found at  $m/z$  636.1160 and 654.1265, respectively. Based on the HRMS data, their structures were determined to be the adduct of methoxylated quercetin and GSH, as well as the adduct of hydrolyzed methoxylated quercetin and GSH. The adduct of  $m/z$  663.1013 was inferred to be an adduct of dimethoxylated quercetin with GSH after dehydrogenation. The mass spectra of the main products are provided in Electronic Supplementary Material Fig. S2A-D.

## Rutin

Rutin is a rutinoside of quercetin including aglycone quercetin, rhamnose, and glucose, which has more abundant active functional groups than quercetin [30]. Similarly, it exhibited a higher ion response intensity in negative ion mode due to its affluent active hydroxyl groups (Fig. 6A), and the response intensity of EIC at  $m/z$  609.1460 significantly decreased after electrochemical oxidation, indicating an electrochemical reaction. The MS spectrum of rutin in negative ion mode is shown in Electronic Supplementary

Material Fig. S1C. The electrochemical method also provided abundant product information for simulating the oxidative metabolism of rutin with the results shown in Fig. 6B. There are four ion peaks with strong response intensities at  $m/z$  593.1515, 623.1619, 691.1504, and 607.1308, which were described as the dehydroxylation product, methylation product, tetramethylation and dihydroxylation followed by dehydrogenation product, and single dehydroxylation product of rutin, respectively. A weak ion peak at  $m/z$  675.1553, which is 16 Da lower than  $m/z$  691.1504, can be explained as the product of tetramethylation and hydroxylation followed by dehydrogenation. In addition, there are also five weaker ion peaks at  $m/z$  653.1731, 639.1572, 637.1416, 655.1523, and 669.1680. The  $m/z$  value of 639.1572 was 30 Da higher than the prototype compound which may be caused by methoxylation of rutin. The  $m/z$  value of 637.1416 was 28 Da higher than rutin and speculated as dehydrogenation after methoxylation of rutin. The  $m/z$  values of 653.1731 and 655.1523 were 14 Da and 16 Da higher than methoxylated rutin ( $m/z$  639.1572), indicating further methylation or hydroxylation of methoxylated rutin. According to the results of HRMS,  $m/z$  669.1680 can be inferred as further hydroxylation of  $m/z$  653.1731 or methylation of  $m/z$  655.1523.

The electrochemical method also provides possibilities for the study of the adduct metabolites produced by the addition of active oxidation products (phase I oxidative metabolites) and GSH. Potential adducts between the electrochemical oxidation products of rutin and GSH were identified by EIC spectra. As shown in Fig. 6C, the ion peak of  $m/z$  914.2175 was presumed to be formed by the adduct of rutin

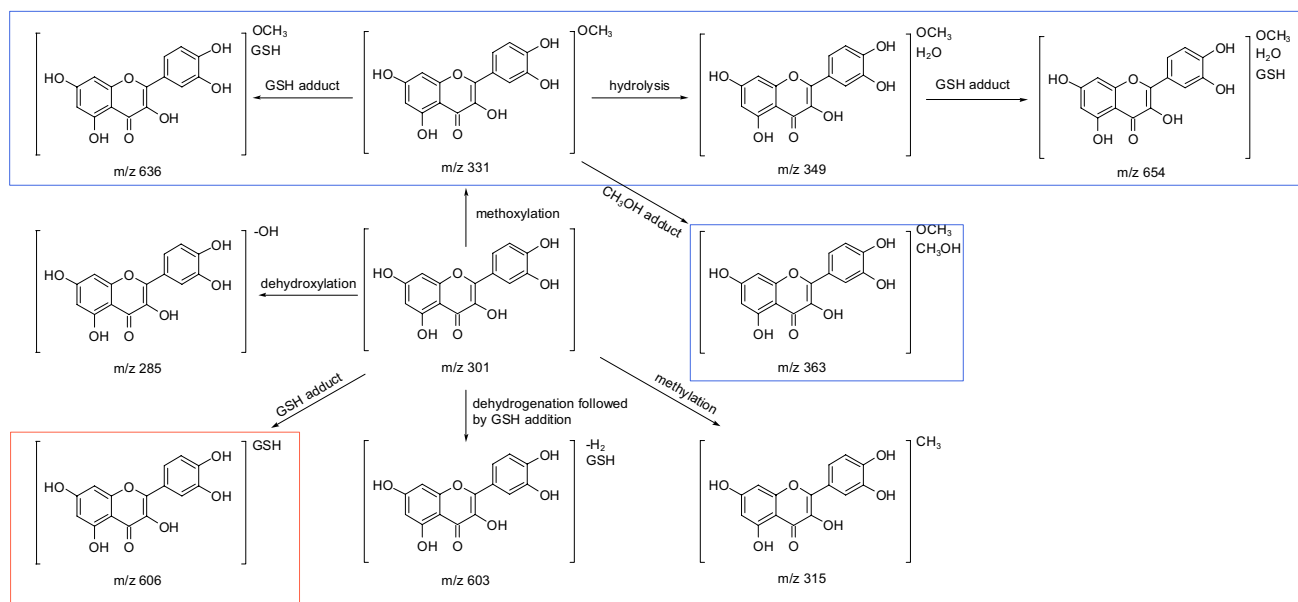


**Fig. 8** Metabolic pathway of quercetin in simulated metabolism



and GSH. The signal of  $m/z$  944.2275 may attribute to the combination form of GSH and methoxylated rutin. There was also a high intensity extracted ion peak of  $m/z$  767.1382, which might be interpreted as a covalent compound of GSH and rutin that break bonds to remove rhamnose groups. The mass spectra of the main products are provided in Electronic Supplementary Material Fig. S3A-D.

### Identification of metabolites by liver microsomes

Furthermore, in order to verify the feasibility of simulating the biological metabolism of target substances by using electrochemical methods, conventional *in vitro* incubation metabolism simulation experiments by rat liver microsomes were also carried out. The products EICs and information were obtained by HPLC-MS with the results shown in Fig. 7. Based on the accurate molecular weight from high-resolution mass spectrometry, the *in vitro* incubated phase I and phase II metabolites of flavone, quercetin, and rutin

were inferred in sequence. As a result of absence of active functional groups in flavone, no metabolites were observed in both phase I and phase II metabolism except for flavone, which was consistent with the results of the electrochemical simulation mentioned above. Quercetin and rutin, on the other hand, showed metabolic activity *in vitro* during liver microsomes incubation experiments.

In phase I metabolic process, the *in vitro* incubation of quercetin by rat liver microsomes exhibited partially identical products to the electrochemical simulation (including  $m/z$  285.0408 and 315.0514 shown in Fig. 7A, corresponding to dehydroxylation and methylation products respectively) with strong response strength, indicating an identical pathway as the electrochemical simulation process. However, no methoxylation and other related products, such as  $m/z$  331.0450, 349.0556, and 363.0713, were detected. Also the *in vitro* incubation products of rutin showed partial similarities with the electrochemical simulation products, such as methylation and hydroxylation products (Fig. 7B), but its

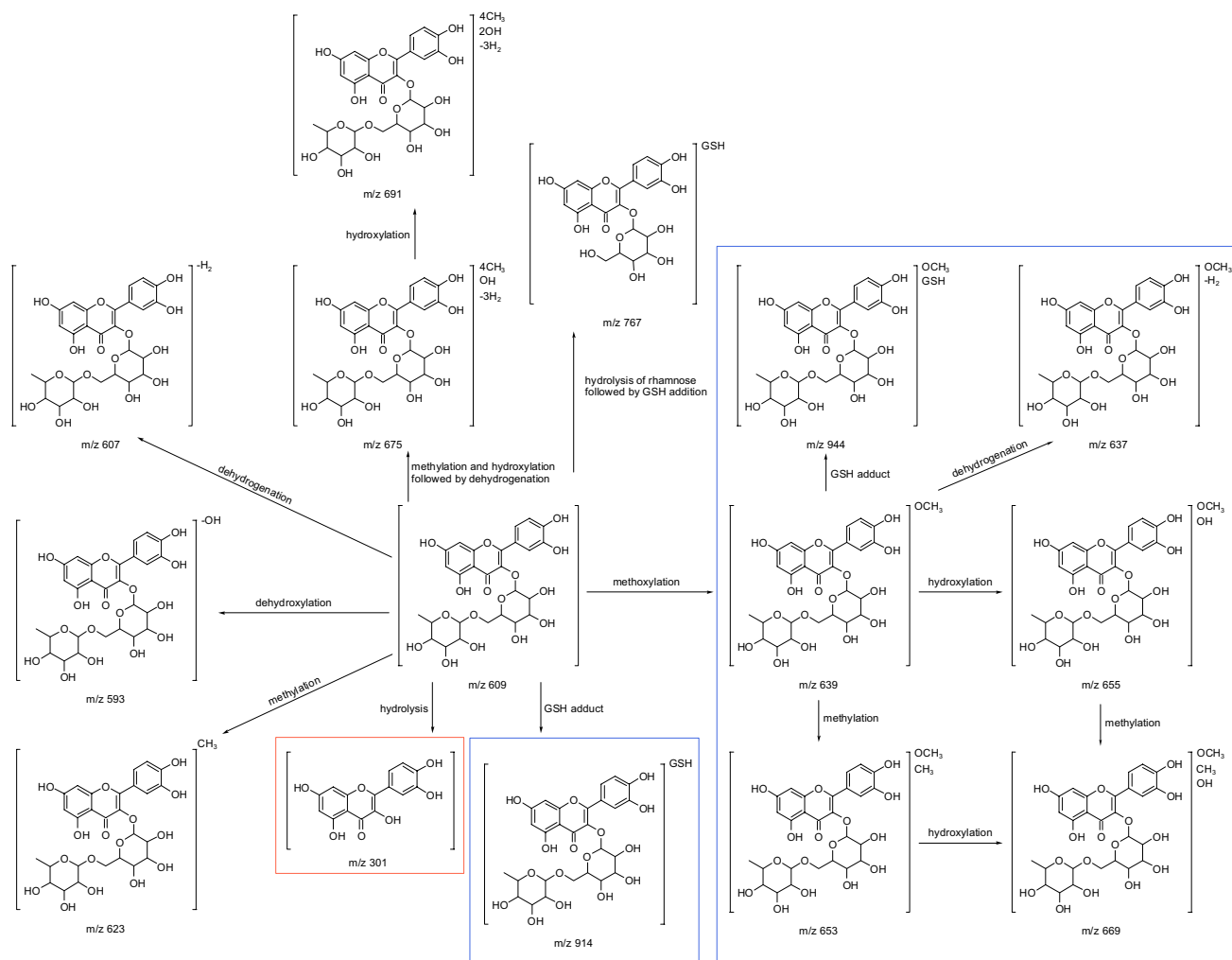


Fig. 9 Metabolic pathway of rutin in simulated metabolism

methoxylation and related products were not detected in the *in vitro* incubation experiment. However, the main product of this metabolic process was quercetin ( $m/z$  301.0345), the hydrolysis product of rutin, which was not found in the products of electrochemical simulation metabolism.

In phase II metabolic process, the *in vitro* incubation of quercetin exhibited different metabolites. In addition to the same metabolite as the electrochemical simulation ( $m/z$  603.0796), new metabolite was also discovered at 606.1041 (Fig. 7C), which was belonging to the adduct of quercetin prototype and GSH. The types of phase II metabolites of rutin were significantly less than those of electrochemical simulation products. As shown in Fig. 7D, except for a small amount of GSH conjugation with rhamnose removed rutin ( $m/z$  767.1382), the main product was the hydrolysis product quercetin ( $m/z$  301.0345). By comparison, it was found that simulation of metabolism of flavonoid small molecules (flavone, quercetin, and rutin) using electrochemical methods resulted in a more diverse variety of metabolites than that of *in vitro* incubation by liver microsomes, which was consistent with the results reported in the literature [12]. However, due to the varying catalytic activity of coenzymes towards different substrates, metabolic reactions in liver microsomes may lead to different metabolites or product concentration, which can also explain why some metabolites or metabolic pathways are missing in liver microsomes metabolism. The mass spectra of the main products are also served in Electronic Supplementary Material Fig. S4A-F.

Based on the above experimental results, the possible metabolic pathways and metabolites of quercetin and rutin in electrochemical simulation and *in vitro* incubation by liver microsomes were speculated with the results shown in Fig. 8 and Fig. 9 (the blue labeled products were only found in electrochemical simulation, while the red labeled products were only found in liver microsomes incubation), respectively, and some of the metabolites were consistent with literature reports [31, 32].

## Conclusion

In this study, a simple and efficient approach was designed to explore the oxidation behavior and potential simulated metabolites of flavone, quercetin, and rutin. Electrochemistry, as a flexible, fast, and efficient technology, can be a good choice for simulating oxidative metabolism of living organisms *in vitro*. HPLC-MS analysis combines the advantages of excellent separation ability of chromatography and high sensitivity detection of mass spectrometry, enabling real-time online analysis of possible metabolism and products of electrochemistry. The results indicated that the

metabolic products obtained by electrochemical simulation were more abundant than those obtained by microsomes incubation, which also avoided the complex pretreatment process of the sample. The presented method provides a feasible reference model for achieving high-throughput and rapid *in vitro* simulation of metabolism and analysis of more types of substrates.

**Supplementary Information** The online version contains supplementary material available at <https://doi.org/10.1007/s00216-024-05227-7>.

**Author contribution** Yanyan Niu: conceptualization, methodology, validation, formal analysis, investigation, visualization, data curation and writing, original draft, review, and editing. Yuxue Chen: validation, visualization, investigation, formal analysis, and methodology. Juan Zhou: methodology, investigation, formal analysis, validation, and resources. Wei Sun: resources, funding acquisition, project administration, review, and editing.

**Funding** The work was supported by the Specific Research Fund of the Innovation Platform for Academicians of Hainan Province (YSPTZX202126), Hainan Provincial Natural Science Foundation of Youth Fund Project (221QN0879).

## Declarations

**Competing interests** The authors declare no competing interests.

## References

1. Herl T, Matysik FM. Recent developments in electrochemistry-mass spectrometry. *ChemElectroChem*. 2020;7:2498–512.
2. Mekonnen TF, Panne U, Koch M. Electrochemistry coupled online to liquid chromatography-mass spectrometry for fast simulation of biotransformation reactions of the insecticide chlorpyrifos. *Anal Bioanal Chem*. 2017;409:3359–68.
3. Mekonnen TF, Panne U, Koch M. Glucosylation and glutathione conjugation of chlorpyrifos and fluopyram metabolites using electrochemistry/mass spectrometry. *Molecules*. 2019;24:898–909.
4. Chen Y, Xie Y, Li L, Wang Z, Yang L. Advances in mass spectrometry imaging for toxicological analysis and safety evaluation of pharmaceuticals. *Mass Spectrom Rev*. 2023;42:2207–33.
5. Attwa MW, AlRabiah H, Mostafa GAE, Kadi AA. Development of an LC-MS/MS method for quantification of sapitinib in human liver microsomes: *in silico* and *in vitro* metabolic stability evaluation. *Molecules*. 2023;28:2322–37.
6. Sun X, Ye Y, Sun J, Tang L, Yang X, Sun X. Advances in the study of liver microsomes in the *in vitro* metabolism and toxicity evaluation of foodborne contaminants. *Crit Rev Food Sci Nutr*. 2022. <https://doi.org/10.1080/10408398.2022.2131728>.
7. Herl T, Matysik FM. Investigation of the electrooxidation of thymine on screen-printed carbon electrodes by hyphenation of electrochemistry and mass spectrometry. *Anal Chem*. 2020;92:6374–81.
8. Sagandykova G, Walczak-Skierska J, Monedeiro F, Pomastowski P, Buszewski B. New methodology for the identification of metabolites of saccharides and cyclitols by off-line EC-MALDI-TOF-MS. *Int J Mol Sci*. 2020;21:5256–75.

9. Faber H, Vogel M, Karst U. Electrochemistry/mass spectrometry as a tool in metabolism studies—a review. *Anal Chim Acta*. 2014;834:9–21.
10. Yang J, Dong X, Zhen XT, Chen Y, Zheng H, Ye LH, Liu FM, Cao J. Rapid analysis and identification of flavonoid and organic acid metabolites in Hawthorn using an on-line flow injection assisted electrochemical microreactor combined with quadrupole time-of-flight tandem mass spectrometry. *J Food Compos Anal*. 2021;96:103700.
11. Szultka-Mlynska M, Buszewski B. Electrochemical oxidation of selected immunosuppressants and identification of their oxidation products by means of liquid chromatography and tandem mass spectrometry (EC-HPLC-MS/MS). *J Pharmaceut Biomed Anal*. 2019;176:112799–809.
12. Yue ZX, Gu YX, Yan TC, Liu FM, Cao J, Ye LH. Phase I and phase II metabolic studies of Citrus flavonoids based on electrochemical simulation and *in vitro* methods by EC-Q-TOF/MS and HPLC-Q-TOF/MS. *Food Chem*. 2022;380:132202.
13. Shen N, Wang T, Gan Q, Liu S, Wang L, Jin B. Plant flavonoids: classification, distribution, biosynthesis, and antioxidant activity. *Food Chem*. 2022;383:132531.
14. Batiha GES, Beshbishy AM, Ikram M, Mulla ZS, El-Hack MEA, Taha AE, Algammal AM, Elewa YHA. The pharmacological activity, biochemical properties, and pharmacokinetics of the major natural polyphenolic flavonoid: quercetin. *Foods*. 2020;9:374–89.
15. Jucá MM, Filho FMSC, de Almeida JC, da Mesquita DS, de Bariga JRM, Dias KCF, Barbosa TM, Vasconcelos LC, Leal LKAM, Ribeiro JE, Vasconcelos SMM. Flavonoids: biological activities and therapeutic potential. *Nat Prod Res*. 2020;34:692–705.
16. Shamsudin NF, Ahmed QU, Mahmood S, Shah SAA, Khatib A, Mukhtar S, Alsharif MA, Parveen H, Zakaria ZA. Antibacterial effects of flavonoids and their structure-activity relationship study: a comparative interpretation. *Molecules*. 2022;27:1149–91.
17. Kim CJ, Cho SK. Pharmacological activities of flavonoids (III) structure-activity relationships of flavonoids in immunosuppression. *Arch Pharm Res*. 1991;14:147–59.
18. Stanley LA. Drug metabolism. In: McCreath SB, Clement YN, editors. *Pharmacognosy*. New York: Academic Press; 2024. p. 597–624.
19. Müller L, Keuter L, Bücksteeg D, Uebel T, Wilken M, Schürmann L, Behrens M, Humpf HU, Esselen M. Metabolic conjugation reduces *in vitro* toxicity of the flavonoid nevadensin. *Food Chem Toxicol*. 2022;164:113006.
20. Lai Y, Chu X, Di L, Gao W, Guo Y, Liu X, Lu C, Mao J, Shen H, Tang H, Xia CQ, Zhang L, Ding X. Recent advances in the translation of drug metabolism and pharmacokinetics science for drug discovery and development. *Acta Pharm Sin B*. 2022;12:2751–77.
21. Doytchinova I. Drug design—past, present, future. *Molecules*. 2022;27:1496–504.
22. Pantaleão SQ, Fernandes PO, Gonçalves JE, Maltarollo VG, Honorio KM. Recent advances in the prediction of pharmacokinetics properties in drug design studies: a review. *ChemMedChem*. 2022;17:e202100542.
23. Li S, Yu L, Shi Q, Liu Y, Zhang Y, Wang S, Lai X. An insight into current advances on pharmacology, pharmacokinetics, toxicity and detoxification of aconitine. *Biomed Pharmacother*. 2022;151:113115.
24. Richter EM, Munoz RAA. Amperometric detection for bioanalysis. In: Kubota LT, Silva JAFd, Sena MM, Alves WA, editors. *Tools and trends in bioanalytical chemistry*. Switzerland: Springer Cham; 2022. pp. 253–64.
25. Zheng Q, Wang Z, Xiong A, Hu Y, Su Y, Zhao K, Yu Y. Elucidating oxidation-based flavour formation mechanism in the aging process of Chinese distilled spirits by electrochemistry and UPLC-Q-Orbitrap-MS/MS. *Food Chem*. 2021;355:129596.
26. Beutler E. Nutritional and metabolic aspects of glutathione. *Annu Rev Nutr*. 1989;9:287–302.
27. Guan X. Glutathione and glutathione disulfide—their biomedical and pharmaceutical applications. *Med Chem Res*. 2023;32:1972–94.
28. Pfaff AR, Beltz J, King E, Ercal N. Medicinal thiols: current status and new perspectives. *Mini-Rev Med Chem*. 2020;20:513–29.
29. Farina M, Aschner M. Glutathione antioxidant system and methylmercury-induced neurotoxicity: an intriguing interplay. *BBA-Gen Subjects*. 2019;1863:129285.
30. Magar RT, Sohng JK. A review on structure, modifications and structure-activity relation of quercetin and its derivatives. *J Microbiol Biotechnol*. 2020;30:11–20.
31. van der Woude H, Boersma MG, Vervoort J, Rietjens IMCM. Identification of 14 quercetin phase II mono- and mixed conjugates and their formation by rat and human phase II *in vitro* model systems. *Chem Res Toxicol*. 2004;17:1520–30.
32. Zhang Y, Ouyang L, Mai X, Wang H, Liu S, Zeng H, Chen T, Li J. Use of UHPLC-QTOF-MS/MS with combination of *in silico* approach for distributions and metabolites profile of flavonoids after oral administration of Niu Huang Shangqing tablets in rats. *J Chromatog B*. 2019;1114–1115:55–70.

**Publisher's Note** Springer Nature remains neutral with regard to jurisdictional claims in published maps and institutional affiliations.

Springer Nature or its licensor (e.g. a society or other partner) holds exclusive rights to this article under a publishing agreement with the author(s) or other rightsholder(s); author self-archiving of the accepted manuscript version of this article is solely governed by the terms of such publishing agreement and applicable law.